

# The Impact of Clay Loading on the Relative Intercalation of Poly(Vinyl Alcohol)-Clay Composites

Moustafa M. Zagho<sup>1,2\*</sup>, Mahmoud M. Khader<sup>3</sup>

<sup>1</sup>Center for Advanced Materials, Qatar University, Doha, Qatar

<sup>2</sup>Materials Science and Technology Master Program, College of Arts and Science, Qatar University, Doha, Qatar

<sup>3</sup>Gas Processing Center, College of Engineering, Qatar University, Doha, Qatar

Email: \*moustafa.zagho1985@gmail.com

**How to cite this paper:** Zagho, M.M. and Khader, M.M. (2016) The Impact of Clay Loading on the Relative Intercalation of Poly(Vinyl Alcohol)-Clay Composites. *Journal of Materials Science and Chemical Engineering*, 4, 20-31.

<http://dx.doi.org/10.4236/msce.2016.410003>

**Received:** September 8, 2016

**Accepted:** October 8, 2016

**Published:** October 11, 2016

Copyright © 2016 by authors and Scientific Research Publishing Inc. This work is licensed under the Creative Commons Attribution International License (CC BY 4.0).

<http://creativecommons.org/licenses/by/4.0/>



Open Access

## Abstract

Polymer clay nanocomposites (PCN) materials are industrially applied because of their unique properties. However many of their physical and chemical properties have not been determined. The formed structures of polymer/clay nanocomposite depend on the nature of interactions between polymer chains and clay platelets. According to the possible modes of interactions between polymer matrix and clay sheets, these nanocomposites can be classified into: intercalated, flocculated and exfoliated nanocomposites. In this work, the morphology of the nanocomposite was studied using X-ray diffraction (XRD) and nanoscaning electron microscopy (NSEM). XRD and NSEM measurements confirmed the intercalation between poly(vinyl alcohol) chains and cloisite® 20A sheets. Because of the intercalation between the clay platelets and the PVA chains, as the clay concentration increases as the band intensities in FT-IR spectra increase. On the other hand, the XRD did not provide clear shift of any of the clay peaks for PVA/cloisite® 10A nanocomposites and confirm the non-intercalation between PVA matrix and cloisite® 10A platelets. The relative intercalation (RI) of PVA/Cloisite® 20A nanocomposites declined with increase in the clay loadings. In contrast, for PVA/Cloisite® 10A, RI values slightly increased with increasing the clay loading.

## Keywords

Poly(Vinyl Alcohol), Cloisite, Nanocomposites, Relative Intercalation, FT-IR Spectra

## 1. Introduction

Polymers are hardly used in their pure form in industrial applications; therefore they

are vastly modified with fillers like fire retardants, plasticizers, colorants and organotin compounds. The nanocomposite materials are critically important from both the academic and industrial point of views. Many of the recently published literatures are focusing on polymer-nanoclay composite materials due to its performance characteristics.

The fabrication of polymer nanocomposites is an integral aspect of polymer nanotechnology. By inserting the nanometric inorganic fillers, the properties of polymers will be improved; consequently, several industrial applications have been initiated depending on the inorganic material added to the polymers. Solution technique is one of the most common and less time consuming methods for the preparation of polymer nanocomposites. Polymer nanocomposites are structures in which nanoscopic inorganic particles, typically 10 - 100 Å in at least one dimension, are finely dispersed in an organic polymer chains to modify the thermal and mechanical properties of the polymer.

Structures in which the inorganic particles are the individual layers of a lamellar compound like smectite clay or a nanocomposite of a polymer (such as nylon) embedded among layers of silicates exhibit different physical characteristics relative to the pure polymer. A case in point, polymer-silicate nanocomposites have stiffness, strength, and dimensional stability in two dimensions rather than one. Because of nanometer length scale which minimizes scattering of light, nanocomposites are usually transparent. Polymer nanocomposites offer a new alternative to traditional polymers. Filler dispersion nanocomposites exhibit significantly improved when compared to the pristine polymers or their conventional composites because of their nanometer sizes.

In these materials, nanofillers are dispersed in polymer network providing improvement in the performance characteristics of the pristine polymer. Nanocomposite materials consisting of inorganic nanolayers of montmorillonite (MMT) clay and organic polymers have unique characteristics like thermal [1], mechanical [2], molecular barrier [3], flame retardant [4] and corrosion protection properties [5]-[7] of polymers at low clay loading compared to polymer composites containing common fillers and these properties can be noticed when two dissimilar chemical components combine at the molecular level.

There are many factors influencing the final characteristics of the nanocomposites which are filler aspect ratio, filler particle size, filler dispersion, filler alignment and orientation, and polymer-polymer and polymer-filler interfacial interactions. Smectite class of aluminum silicate clays is one of the most significant fillers for polymers, of which the most used is MMT. MMT has been implemented with several polymers industry as it has a potentially high aspect ratio and high surface area that could make excellent improvement in the performance characteristics of the polymer and it is environmentally friendly, naturally occurring, and readily available in large quantities. Due to their pure state which is hydrophilic, the nanolayers are not easily dispersed in most polymers and tend to form agglomerates. To overcome the dispersive problems, researchers have modified the natural clays by adding some organic materials. In addi-

tion, these modified polymers produce well-organized nanocomposites. MMT forms stable suspensions in water and good dispersion of these inorganic crystalline platelets in water soluble polymers, such as poly(vinyl alcohol) and poly(ethylene oxide). In this paper, PVA-Cloisite® 20A and PVA-Cloisite® 10A nanomposites are studied. Moreover, this paper includes a study of the effect of clay concentration on the relative intercalation of poly(vinyl alcohol)-clay nanocomposites.

## 2. Methodology

### 2.1. Source of Chemicals and Materials

PVA was purchased from Sigma-Aldrich. Cloisite® 20A and cloisite® 10A were purchased from Southern Clay Products and used in the preparations without any modification. For cloisite® 20A, the quaternary ammonium used as an organic modifier for the clays is dimethyl, dihydrogenated tallow (2M2HT), where HT stands for a tallow-based compound (~65% C18, ~30% C16, ~5% C14) in which a majority of the double bonds have been hydrogenated. The modifier concentration of cloisite® 20A is 95 mequiv/100 g clay. Cloisite® 10A contains dimethyl, benzyl, hydrogenated tallow, quaternary ammonium salt (2MBHT). The modifier concentration of cloisite® 10A is 125 mequiv/100 g clay. Ethanol (95.1% - 96.9% Riedel-deHaen).

### 2.2. Synthesis of Polymer Nanocomposites (PNCs) Using Solution Technique

PCN materials can be prepared using different techniques. In this article, poly(vinyl alcohol)-clay nanocomposite (PVACN) materials were fabricated using solution method. This synthesis helped in dispersing the inorganic nanolayers of MMT sheets homogeneously in PVA network and the PVA chains between MMT silicate layers. In this technique, PVA was dissolved first in deionized water by heating at 60°C, the clays were dispersed in a solution of water and ethanol (in a 3:2 volume ratio). PVACN material was fabricated by adding the clay suspension to the dissolved PVA in different quantities that gave varied wt% clay loadings on the final product with continuous stirring at 60°C for 2 hr. The mixture was then left to dry out at 40°C for several days. Then the resulted PVACN materials were finely grinded into powders using cryomil grinder in which the sample was cooled down in liquid nitrogen. The cold PVACN materials were grinded at a frequency of 0.5 Hz for 20 minutes [8]. Finally, the formed compounds can be used for morphology measurements including XRD, NSEM, and FT-IR.

## 3. Instruments and Methodology

### 3.1. X-Ray Diffraction (XRD)

XRD is used to determine the crystal structures of various solids, including lattice constants, orientation of single crystals, and crystal defects. Wide angle XRD of the PCN materials was performed by using Rigaku Mini Flex II X-ray Diffractometer equipped with Cu-K $\alpha$  source ( $\lambda = 1.5404 \text{ \AA}$ ). It was operated at 30 kV and 10 mA and scans were obtained in a  $2\theta$  range from 2° to 30°, with a scan speed of 0.5°/minute. The basal in-

ter-planar spacing  $d$  is calculated by the Bragg's law ( $n\lambda = 2d \sin\theta$ ) where  $n$  is an integer,  $\lambda$  is the wavelength of incident wave (1.5404 Å), and  $\theta$  is the angle between the incident X-ray and the scattering planes. A relative intercalation (RI) of the clay in the polymeric matrix has been computed as a percentage increase of the  $d$ -spacing according to the following equation:

$$RI = \frac{d - d_o}{d_o} \times 100$$

where,  $d_o$  is the  $d$ -spacing of the pristine clay and  $d$  is the  $d$ -spacing of the clay in the nanocomposites.

### 3.2. Nano Scanning Electron Microscopy (NSEM)

NSEM "NOVA NANOSEM 450" was employed to study the surface morphology of PVA, pristine clays, and PCN materials. The PVA, clays, and PVACN were both dispersed in water before spreading over the SEM holder, also were coated by a thin film of gold after drying out. Coating of dry samples with a thin film of gold was performed in a gold sputtering chamber. This technique was employed by voltage of 500 V to 30 KV.

### 3.3. Fourier Transform Infrared Spectroscopy (FT-IR)

Fourier Transform Infrared (FT-IR) spectroscopy is used to identify functional groups of organic or inorganic compound. FTIR analysis was conducted using the BX Perkin Elmer-FTIR Spectrometer. The samples were grounded with KBr powder. The powdered mixture was then filled into a press where a thin and transparent pellet was made. The pellets were placed into the sample holder for scanning.

## 4. Results and Discussion

### 4.1. Structural Morphology (XRD & SEM)

The morphology of the clay-containing PVA systems was evaluated using a combination of XRD and NSEM. The XRD analysis and SEM observations are used to study the dispersion and exfoliation of nanoparticles. XRD analysis determined the interlayer spacing of the silicate layers in the original layered silicates and in the intercalated nanocomposites. NSEM defined qualitatively the internal structure, spatial distribution and dispersion of the nanoparticles within the polymer matrix.

The value of  $2\theta$  in the XRD pattern enables one to evaluate the  $d$ -spacing of the intercalated structures, by evaluating how much expansion has occurred due to penetrating the polymer chains into the silicate layers of the clay where the  $d$ -spacing of the intercalated structures are calculated using Bragg's equation. There are three possibilities: 1) no change in the  $d$ -spacing of the clay, indicating no dispersion or no nanocomposite structure formation; 2) the  $2\theta$  shifts to a lower value, which indicates intercalate structures in the nanocomposite where in this case the  $d$ -spacing of the intercalated structures will be higher than that of the pristine clay; or finally 3) the XRD pattern does not exhibit peak or a broad peak, indicating a disordered structure (loss of parallel

clay silicate layers stacking) [9].

The XRD patterns of the Cloisite® 20A powder and nanocomposite powders are shown in **Figure 1**. The peak at  $2\theta = 3.8^\circ$  is attributed to the basal spacing ( $\sim 23 \text{ \AA}$ ) of the Cloisite® 20A. The observed increase in the basal spacing of the PVA/Cloisite® 20A samples explains the formation of intercalated structures, due to the polymer chains penetrating into the clay sheets (**Table 1**). This expansion of the clay's basal spacing is due to strong interactions between the modified clay's surface and the polymer groups via the formation of hydrogen bonding with the clay platelets [8].

It should be noted that there is a decrease of the clay's basal spacing of Cloisite® 20A in PVA-Cloisite® 20A composites as the clay loading increases from 5 wt% to 30 wt% as shown in the **Figure 1** and this can be due to that the polymer chains concentration decreases from 95 wt% to 70 wt% respectively, so the polymer chains can't penetrate into the clay galleries and lead to weak intercalations.

Contrary to PVA/Cloisite® 20A PNC, the XRD of PVA/Cloisite® 10A clay mixture did not show significant shift of any of the clay's XRD peaks due to adding PVA; indicating that Cloisite® 10A did not intercalate with the PVA chains. Because the molecular

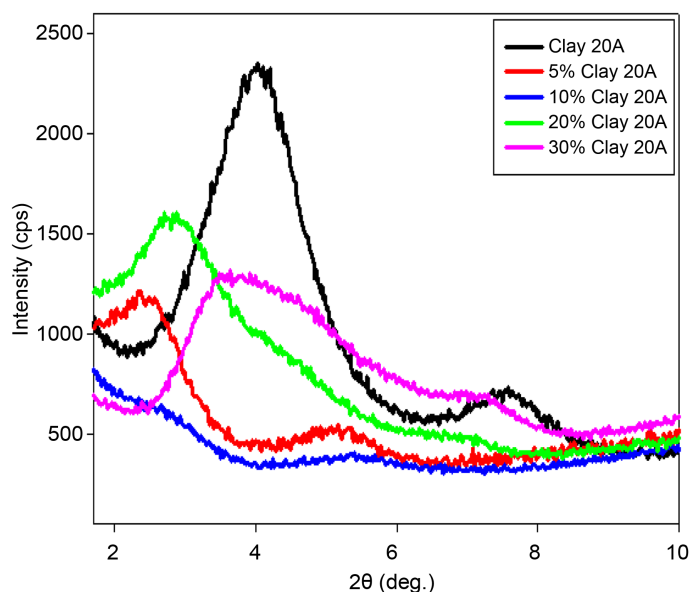


**Figure 1.** XRD patterns of Cloisite® 20A and PVA/Cloisite® 20A at clay loading of 5 wt% - 30 wt%.

**Table 1.** *d*-spacing of Cloisite® 20A in PVA composites at loading rate of 5 wt% - 30 wt%.

Sample	$2\theta$ (deg.)	<i>d</i> -spacing (Å)
Cloisite® 20A	3.80	23.2
PVA/Cloisite® 20A, 5%	2.50	35.3
PVA/Cloisite® 20A, 10%	2.67	33.0
PVA/Cloisite® 20A, 20%	2.87	30.8
PVA/Cloisite® 20A, 30%	3.77	23.4

structure of Cloisite® 10A contains a benzyl moiety, it is unlikely to promote the interactions with a polar polymer like PVA, as signified from the XRD results (Figure 2). In this case, the interactions between the clay particles and the polymer were very weak and thus, the polymers could not enter into clay galleries. A phase separated composite was instead formed [8].

It can be seen that there is no increase of the clay's basal spacing of Cloisite® 10A in PVA/Cloisite® 10A composites (Table 2) as the clay loading increases from 5 wt% to 40 wt% and a slight increase of the clay's basal spacing in case of 50 wt% of clay loading as shown in Figure 2. This is due to the polymer chains can't penetrate into the clay galleries where the molecular structure of Cloisite® 10A contains a benzyl moiety leading to poor interactions.

Another important evidence for the intercalation of PVA with Cloisite® 20A is shown from the SEM images. The presented Figures 3-7 show the NSEM of pure PVA, bulk Cloisite® 20A, bulk Cloisite® 10A, PVA/5 wt% Cloisite® 20A nanocomposite, and PVA/5 wt% Cloisite® 10A nanocomposite. Figure 6 shows well-dispersed clay 20A flakes within the polymeric chains. Both the XRD and the SEM results indicated that PVA/Cloisite® 20A composites had structures in which the polymeric matrix were intercalated between the clay platelets resulting in a multilayer morphology, built up with

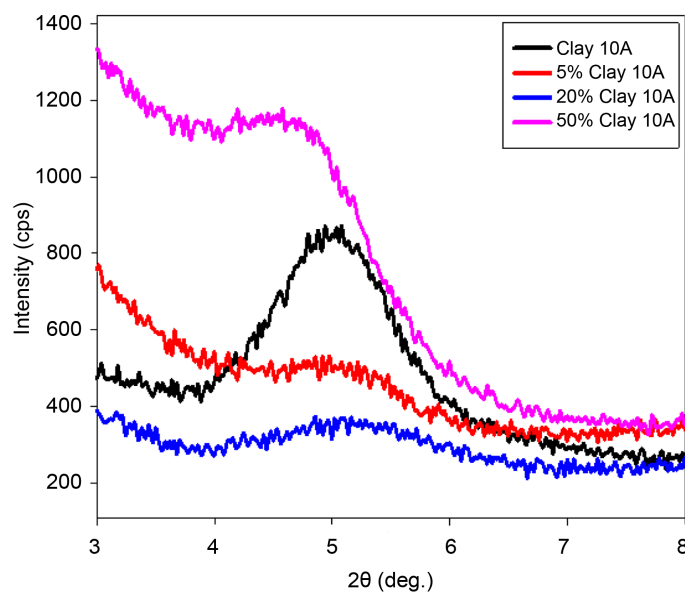
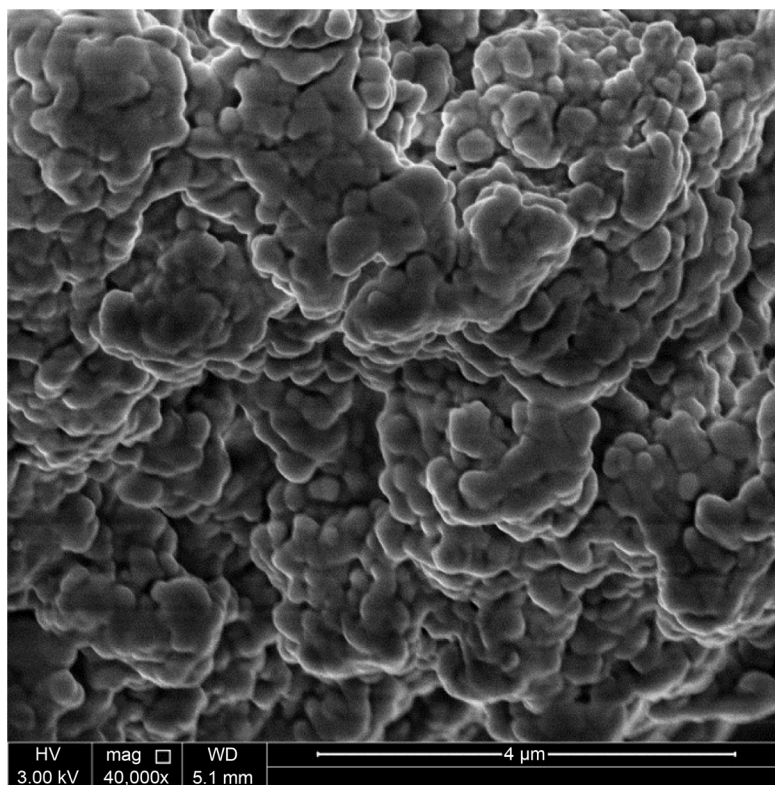


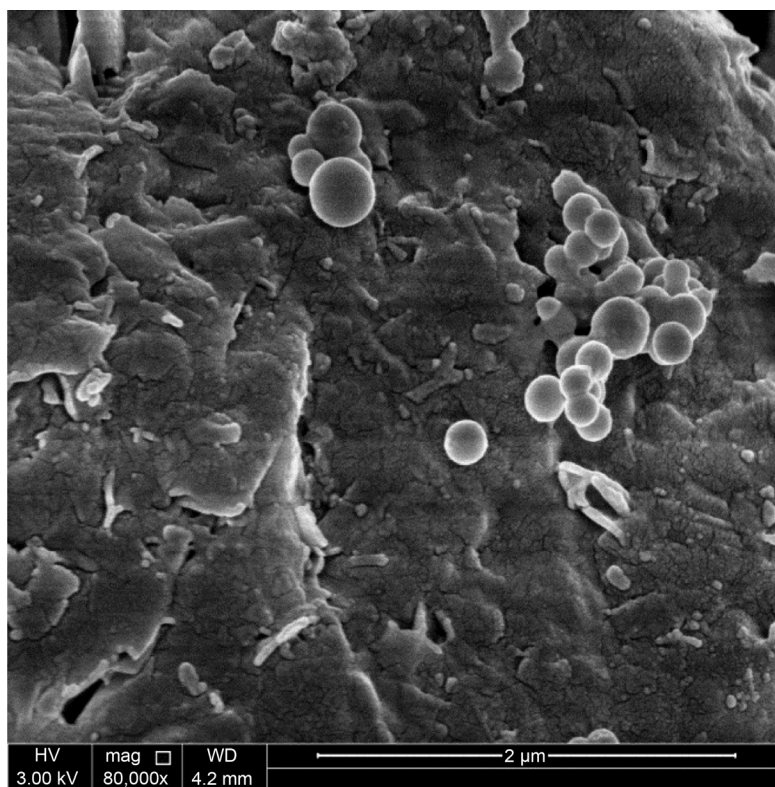
Figure 2. XRD patterns of Cloisite® 10A and PVA/Cloisite® 10A at clay loading of 5 wt% - 50 wt%.

Table 2. *d*-spacing of Cloisite® 10A in PVA composites at loading rate of 5 wt% - 50 wt%.

Sample	2θ (deg.)	<i>d</i> -spacing (Å)
Cloisite® 10A	4.80	18.4
PVA/Cloisite® 10A, 5%	4.80	18.4
PVA/Cloisite® 10A, 20%	4.80	18.4
PVA/Cloisite® 10A, 50%	4.60	19.2



**Figure 3.** NSEM micrograph of the pure PVA.



**Figure 4.** NSEM micrograph of the bulk Cloisite<sup>®</sup> 20A.

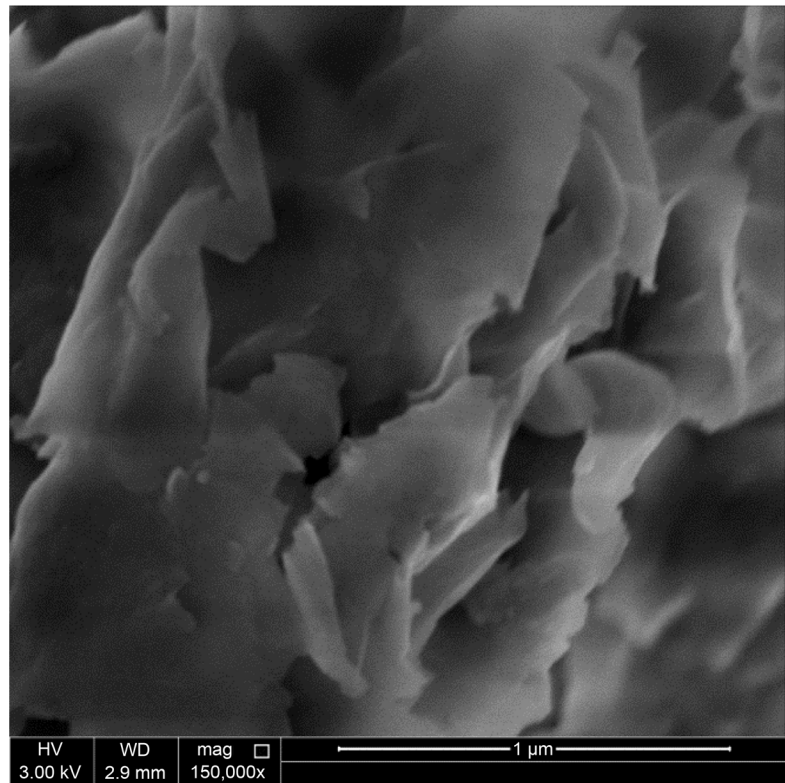


**Figure 5.** NSEM micrograph of the bulk Cloisite® 10A.

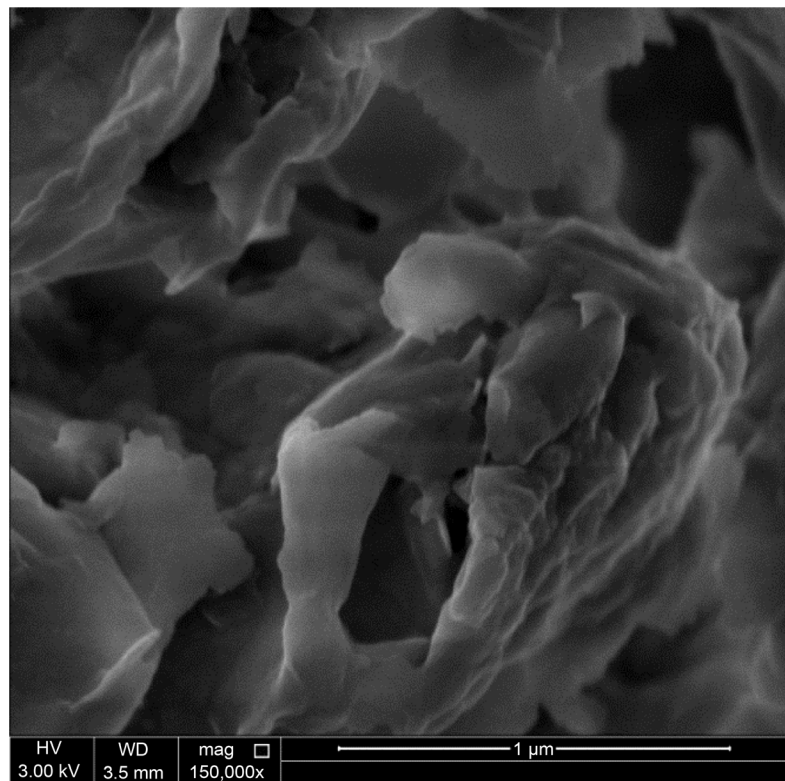


**Figure 6.** NSEM micrograph of PVA/5 wt% Cloisite® 20A nanocomposite.

clay layers, well separated from one another and individually dispersed in the continuous polymer matrix [10].

It should be noted that the characteristic peak of PVA of about  $2\theta = 19.4^\circ$  is not affected when PVA interact with different types of clay such as Cloisite® 20A and Cloisite® 10A and at loading rate of 5 wt% as seen in **Figure 8**.

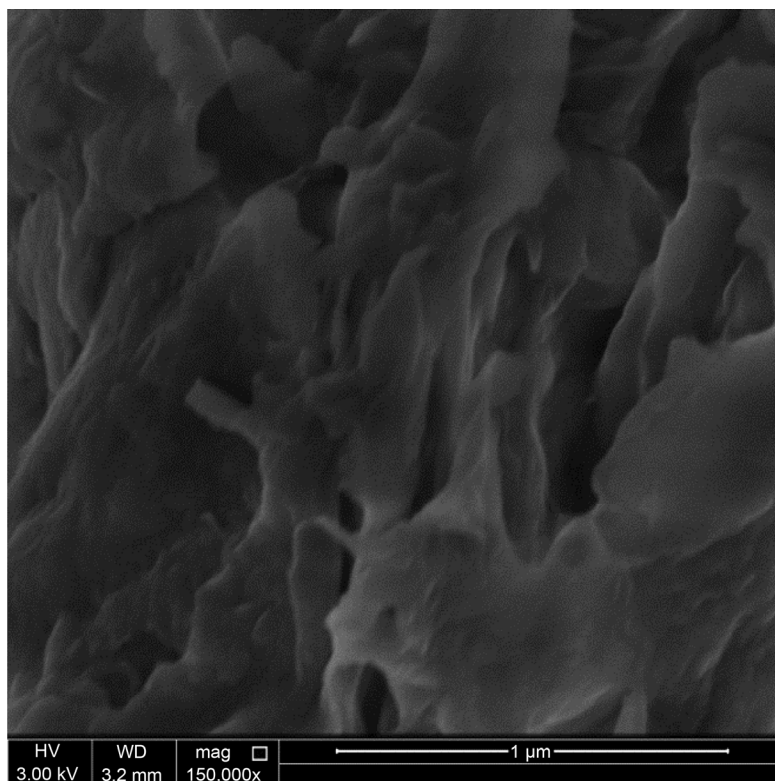


**Figure 7.** NSEM micrograph of PVA/5 wt% Cloisite® 10A nanocomposite.

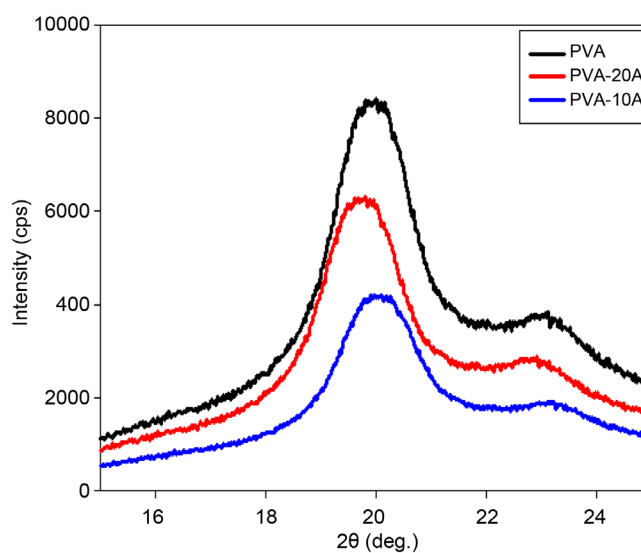


**Figure 8.** XRD patterns of PVA and PVA/clay composites at clay loading of 5 wt%.

The relative intercalations (RI) of PVA/Clay nanocomposites at different clay loading rates are summarized in **Table 3**. For PVA/Cloisite® 20A nanocomposites with increase in clay loading, a decrease in RI was observed. For PVA/Cloisite® 10A, RI values slightly increased with increase in the clay loading. The decrease in the intercalation of Cloisite® 20A could possibly be due to the decrease in the concentration of PVA chains in the nanocomposites which are responsible for the formation of hydrogen bonding with the clay platelets and so resulted in a weak interaction between the polymer matrix and the clay platelets. Whereby the increase in RI of Cloisite® 10A at low concentration of PVA was presumably due to the presence of small crevices in this clay which would have got saturated even with a small amount of added PVA and so the intercalation slightly increases.

#### 4.2. Fourier Transform Infrared (FT-IR) Measurements

The FT-IR spectra of pure PVA, organophilic clay Cloisite® 20A and PCN materials are illustrated in **Figure 9**. The characteristic vibration bands of PVA are shown at 3420  $\text{cm}^{-1}$  (-OH), 2943  $\text{cm}^{-1}$  (-CH<sub>3</sub>), 2891  $\text{cm}^{-1}$  (-CH<sub>2</sub>), 1450  $\text{cm}^{-1}$  (O=C-OR), 1110  $\text{cm}^{-1}$  (C-O-C) and 862  $\text{cm}^{-1}$  (-CH<sub>2</sub>). Due to the intercalation between the clay platelets and the polymer matrix, as the clay loading increases as the band intensities in FT-IR spectra increases [11].

The FT-IR spectra of pure organophilic clay Na-rich MMT and pure Cloisite® 20A are presented in **Figure 10**. It is clear that there are more bands in Cloisite® 20A than Na-rich MMT. These bands were found at 2921.38, 2849.57, 1467.42  $\text{cm}^{-1}$ . Cloisite® 20A is a modified clay of Na-rich MMT, where the quaternary ammonium used as an organic modifier for the clays is dimethyl, dihydrogenated tallow (2M2HT). Therefore, these bands are due to the replacement of Na<sup>+</sup> ion of Na-rich MMT by quaternary ammonium group (2M2HT for Cloisite® 20A) as illustrated in **Figure 10**.

### 5. Conclusion

In this work, the research on different PVA silicate nanocomposites has been presented.

**Table 3.** Relative intercalation (RI) of PVA/clay nanocomposites at different loading rates.

Sample	<i>d</i> -spacing (Å)	RI (%)
Cloisite® 20A	23.2	-
PVA/Cloisite® 20A, 5%	35.3	52.2
PVA/Cloisite® 20A, 10%	33.0	42.2
PVA/Cloisite® 20A, 20%	30.8	32.8
PVA/Cloisite® 20A, 30%	23.4	0.86
Cloisite® 10A	18.4	-
PVA/Cloisite® 10A, 5%	18.4	0
PVA/Cloisite® 10A, 20%	18.4	0
PVA/Cloisite® 10A, 50%	19.2	4.3

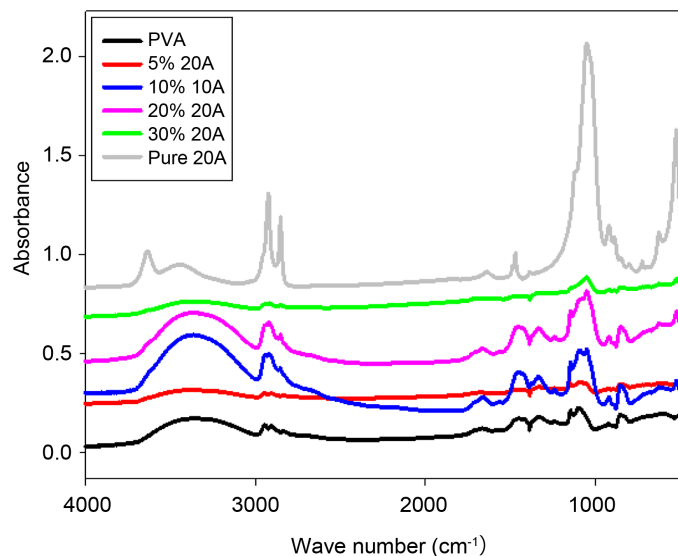


**Figure 9.** Representative FT-IR spectra of PVA, PVA/Cloisite® 20A nanocomposites and bulk Cloisite® 20A.

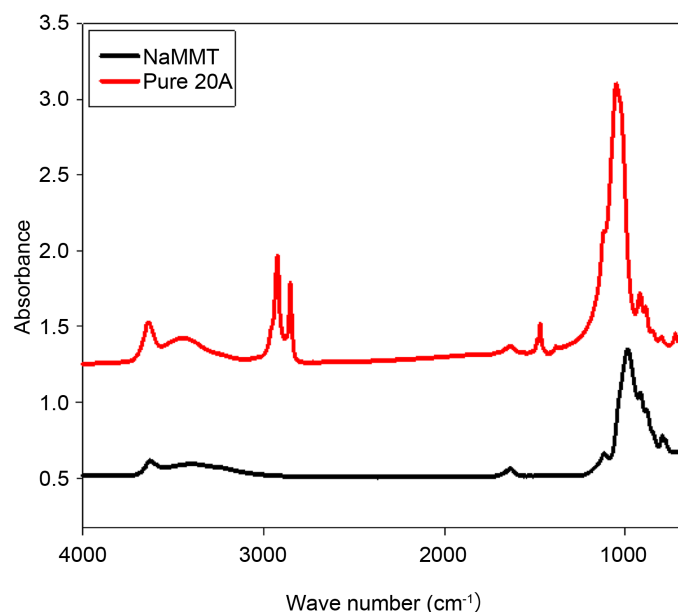


**Figure 10.** Representative FT-IR spectra of pure Na-rich MMT and pure Cloisite® 20A.

Nanocomposites of PVA/Cloisite® 20A, PVA/Cloisite® 10A nanocomposites were synthesized using solution method technique. Solution method was used to prepare a series of PCN with different loadings of layered MMT clay. This preparation technique is used to disperse the inorganic nanolayers of MMT clay in the organic PVA matrix and the PVA polymer chains between the silicate layers of the MMT clay. The intercalation with Cloisite® 20A was evidenced from XRD which showed enlargement of the basal spacing. NSEM also showed that Cloisite® 20A sheets were homogeneously dispersed

within the PVA gallery, presumably, due to intercalation. In FT-IR spectra, because of the intercalation between the clay platelets and the polymer matrix, as the clay loading increases as the band intensities increase. For the second one, PVA/Cloisite® 10A nanocomposites, the XRD did not show significant shift of any of the clay peaks which confirm that there is no intercalation.

## Acknowledgements

The financial support of this research by NPRP Grant # 09-260-1-048 from the Qatar National Research Fund (a member of Qatar Foundation) is gratefully acknowledged.

## References

- [1] Lan, T., Kaviratna, P.D. and Pinnavaia, T.J. (1994) On the Nature of Polyimide-Clay Hybrid Composites. *Chemistry of Materials*, **6**, 573-575. <http://dx.doi.org/10.1021/cm00041a002>
- [2] Tyan, H.-L., Liu, Y.-C. and Wei, K.-H. (1999) Thermally and Mechanically Enhanced Clay/Polyimide Nanocomposite via Reactive Organoclay. *Chemistry of Materials*, **11**, 1942-1947. <http://dx.doi.org/10.1021/cm990187x>
- [3] Wang, Z. and Pinnavaia, T.J. (1998) Nanolayer Reinforcement of Elastomeric Polyurethane. *Chemistry of Materials*, **10**, 3769-3771. <http://dx.doi.org/10.1021/cm980448n>
- [4] Gilman, J.W., Jackson, C.L., Morgan, A.B., Hayyis, J.R., Manias, E., Giannelis, E.P., Wuthenow, M., Hilton, D. and Philips, S.H. (2000) Flammability Properties of Polymer-Layered-Silicate Nanocomposites. Polypropylene and Polystyrene Nanocomposites. *Chemistry of Materials*, **12**, 1866-1873. <http://dx.doi.org/10.1021/cm0001760>
- [5] Yeh, J.-M., Liou, S.-J., Lai, C.-Y., Wu, P.-C. and Tsai, T.-Y. (2001) Enhancement of Corrosion Protection Effect in Polyaniline via the Formation of Polyaniline-Clay Nanocomposite Materials. *Chemistry of Materials*, **13**, 1131-1136. <http://dx.doi.org/10.1021/cm000938r>
- [6] Yeh, J.-M., Chen, C.-L., Chen, Y.-C., Ma, C.-Y., Lee, K.-R., Wei, Y. and Li, S. (2002) Enhancement of Corrosion Protection Effect of Poly(o-Ethoxyaniline) via the Formation of Poly(o-Ethoxyaniline)-Clay Nanocomposite Materials. *Polymer*, **43**, 2729-2736. [http://dx.doi.org/10.1016/S0032-3861\(02\)00005-8](http://dx.doi.org/10.1016/S0032-3861(02)00005-8)
- [7] Yeh, J.-M., Liou, S.-J., Lin, C.-Y., Cheng, C.-Y., Chang, Y.-W. and Lee, K.-R. (2002) Anticorrosively Enhanced PMMA-Clay Nanocomposite Materials with Quaternary Alkylphosphonium Salt as an Intercalating Agent. *Chemistry of Materials*, **14**, 154-161. <http://dx.doi.org/10.1021/cm010337f>
- [8] Al-Marri, M.J., Masoud, M.S., Nassar, A.M.G., Zagho, M.M. and Khader, M.M. (2015) Synthesis and Characterization of Poly(Vinyl Alcohol): Cloisite® 20A Nanocomposites. *Journal of Vinyl and Additive Technology*.
- [9] [www.clays.org](http://www.clays.org)
- [10] Chin, I.-J., Thurn-Albrecht, T., Kim, H.-C., Russell, T.P. and Wang, J. (2001) On Exfoliation of Montmorillonite in Epoxy. *Polymer*, **42**, 5947-5952. [http://dx.doi.org/10.1016/S0032-3861\(00\)00898-3](http://dx.doi.org/10.1016/S0032-3861(00)00898-3)
- [11] Yu, Y.-H., Lin, C.-Y., Yeh, J.-M. and Lin, W.-H. (2003) Preparation and Properties of Poly(Vinyl alcohol)-Clay Nanocomposite Materials. *Polymer*, **44**, 3553-3560. [http://dx.doi.org/10.1016/S0032-3861\(03\)00062-4](http://dx.doi.org/10.1016/S0032-3861(03)00062-4)



**Submit or recommend next manuscript to SCIRP and we will provide best service for you:**

Accepting pre-submission inquiries through Email, Facebook, LinkedIn, Twitter, etc.

A wide selection of journals (inclusive of 9 subjects, more than 200 journals)

Providing 24-hour high-quality service

User-friendly online submission system

Fair and swift peer-review system

Efficient typesetting and proofreading procedure

Display of the result of downloads and visits, as well as the number of cited articles

Maximum dissemination of your research work

Submit your manuscript at: <http://papersubmission.scirp.org/>

Or contact [msce@scirp.org](mailto:msce@scirp.org)